

Pasteurella multocida toxin activates Gβγ dimers of heterotrimeric G proteins

Inga Preuß^{a,b,1}, Barbara Kurig^{c,1}, Bernd Nürnberg^c, Joachim H.C. Orth^a, Klaus Aktories^{a,*}

^a Institut für Experimentelle und Klinische Pharmakologie und Toxikologie, Albert-Ludwigs-Universität Freiburg, Germany

^b Faculty of Biology, Albert-Ludwigs-Universität Freiburg, Germany

^c Institut für Biochemie and Molekularbiologie II, Universität Düsseldorf, and Institut für Experimentelle und Klinische Pharmakologie und Toxikologie, Eberhard-Karls-Universität Tübingen, Germany

ARTICLE INFO

Article history:

Received 14 November 2008

Received in revised form 12 December 2008

Accepted 15 December 2008

Available online 24 December 2008

Keywords:

Heterotrimeric G protein

Gβγ

Gα_q

Pasteurella multocida toxin

PI3-kinase

GTPase cycle

ABSTRACT

The mitogenic *Pasteurella multocida* toxin (PMT) is a major virulence factor of *P. multocida*, which causes *Pasteurellosis* in man and animals. The toxin activates the small GTPase RhoA, the MAP kinase ERK and STAT proteins via the stimulation of members of two G protein families, G_q and G_{12/13}. PMT action also results in an increase in inositol phosphates, which is due to the stimulation of PLCβ via Gα_q. Recent studies indicate that PMT additionally activates Gα_i to inhibit adenylyl cyclase. Here we show that PMT acts not only via Gα but also through Gβγ signaling. Activation of Gβγ by PMT causes stimulation of phosphoinositide 3-kinase (PI3K) γ and formation of phosphatidylinositol-3,4,5-trisphosphate (PIP₃) as indicated by the recruitment of a PIP₃-binding pleckstrin homology (PH) domain-containing protein to the plasma membrane. Moreover, it is demonstrated that Gβγ is necessary for PMT-induced signaling via Gα. Mutants of Gα_q incapable of binding or releasing Gβγ are not activated by PMT. Similarly, sequestration of Gβγ inhibits PMT-induced Gα-signaling.

© 2009 Elsevier Inc. All rights reserved.

1. Introduction

The 146 kDa protein toxin (PMT) from *Pasteurella multocida* is one major virulence factor of the pathogen [1]. Whereas the role of PMT in human *P. multocida*-induced diseases has not been elucidated, the toxin has been shown to cause various diseases of wild-life and domestic animals, including the atrophic rhinitis of pigs, which is characterized by major destruction of the nose turbinate [2,3]. In cell culture of fibroblasts, PMT is one of the most potent mitogens known [4]. PMT stimulates several signaling pathways. The toxin activates the small GTPase Rho, the MAP kinase ERK and STAT proteins [5–7]. These effects are mainly caused by activation of members of two heterotrimeric G protein families, G_q and G_{12/13} [8]. Quite early it was recognized that PMT is a strong stimulator of Gα_q, resulting in phospholipase Cβ activation [4,9]. Notably, Gα₁₁, which couples to same receptors as Gα_q and also activates phospholipase C, is not stimulated by the toxin [8,10]. Stimulation of G proteins by PMT is

independent of coupling to receptors and virtually permanent [11]. More recently, we reported that also Gα_i is potentially activated by PMT [12]. However, the precise molecular mechanism underlying the PMT-induced activation of G proteins is not known. Recently, the crystal structure of a large fragment of PMT, including the biologically active domain, has been solved, suggesting that PMT acts as a cysteine protease [13].

Activation of G proteins by G-protein-coupled receptors (GPCR) causes signaling via Gα and/or Gβγ subunits. However, it has not been shown whether GPCR-independent activation of G proteins by PMT also results in activation of Gβγ and subsequent signaling. Here we report that PMT releases Gβγ from heterotrimeric G proteins, thereby activating the PI3K pathway. Moreover, we demonstrate that Gβγ is necessary for PMT-induced activation of Gα.

2. Experimental procedures

2.1. Materials

Myo-[2-³H]inositol was obtained from Perkin Elmer. All other reagents were of analytical grade and purchased from commercial sources.

2.2. Construction of expression plasmids

Construction of PH domain of general receptor for phosphoinositides-1 (Grp1_{PH}) in pEGFP-C1 [aa 241–386] and p101, p110γ, Gβ₁, Gγ₂,

Abbreviation: F, fluorescence; fMLP, formyl-methionyl-leucyl-phenylalanine; GRK, G-protein-coupled-receptor kinase 1; GRP1, general receptor for phosphoinositides-1; IP, inositol phosphates; MEF, mouse embryonic fibroblasts; PH, pleckstrin homology; PI3K, phosphoinositide 3-kinase; PIP₃, phosphatidylinositol-3,4,5-trisphosphate; PMT, *Pasteurella multocida* toxin; PTX, pertussis toxin.

* Corresponding author. Institut für Experimentelle und Klinische Pharmakologie und Toxikologie, Albertstraße 25, D-79104 Freiburg, Germany. Tel.: +49 761 2035301; fax: +49 761 2035311.

E-mail address: Klaus.Aktories@pharmakol.uni-freiburg.de (K. Aktories).

¹ Indicated authors contributed equally to this work.

flag-NF1-333 (NF1), CFP-GRK2-CT [aa 570-689 of G-protein-coupled-receptor kinase 1] (GRK is also known as β ARK2), phosducin (Pd) and the human formyl-methionyl-leucyl-phenylalanine (fMLP) receptor in pcDNA3 has been described elsewhere [14–17].

2.3. Cell culture, transfection, virus production and transduction

HEK293 cells (from the German Resource Centre for Biological Material) were grown at 37 °C with 5% CO₂ in DMEM with Earle's Salts (Gibco BRL) supplemented with 10% FCS (Gibco BRL), 100 µg/ml streptomycin, and 100 U/ml penicillin (Genaxxon). HEK293 cells stably expressing the muscarinic acetylcholine receptor M₃ [18] were cultured like HEK293 wild-type cells, but in the presence of G418 (0.5 mg/ml). For confocal analysis, cells were seeded on glass cover slips two days prior to transfection. All transfections were done with a calcium phosphate-based transfection method. HEK293 cells were transfected with 0.2 µg of plasmid encoding a formyl-methionyl-leucyl-phenylalanine (fMLP) receptor, 0.4 µg of each of the plasmids encoding the PI3K subunits and the fluorescent PH domain, 1.0 µg of each of the plasmids encoding G β ₁ and G γ ₂ and 1.1 µg each of the plasmids encoding NF1 and GRK2-CT. The total amount of transfected cDNA was always kept constant (2.5 µg/well) by the addition of empty expression vector. All experiments were performed at least 24 h after transfection in serum-starved cells.

Mouse embryonic fibroblasts (MEF) derived from G α_q /G α_{11} -gene deficient or wild-type (wt) mice were cultured as described before [19]. The retroviral vector was produced as described before [20]. In brief, HEK-293T cells were co-transfected with pMD-G, pMD-g/p and the retroviral transfer vector. The calcium phosphate method was used. The supernatant was collected after 3 days and centrifuged to spin down cellular debris. The virus-containing medium was filtered. Cells were infected in the presence of Polybrene. The expression was monitored by Western-blot analysis. Additional transfection of α_{1b} -adrenoceptor expression plasmid was done with the Nucleofection system (Amaxa Biosystems), according to the general protocol for nucleofection of mouse embryonic fibroblasts.

2.4. Confocal laser scanning microscopy

Cell imaging was established and performed as described previously with modifications outlined below [14,21,22]. Glass coverslips were mounted on a custom-made chamber and covered with 200 µl of HEPES-buffered solution (HBS), containing 138 mM NaCl, 6 mM KCl, 1 mM MgCl₂, 1 mM CaCl₂, 5.5 mM glucose, and 10 mM HEPES, pH 7.5. For confocal imaging, an inverted confocal laser scanning microscope with a Plan-Apochromat 63/1.4 objective (model LSM 510-Meta; Carl Zeiss MicroImaging Inc.) was used. To maintain a constant temperature of 37 °C for live cell imaging, the confocal microscope device was equipped with a ZEISS Incubator XL. GFP and Alexa633 were excited at 488 nm and 633 nm, and the fluorescence emission was detected through a 505–530 nm band pass filter and a 650 nm long pass filter, respectively. The pinholes were adjusted to yield optical sections of 0.5–1.0 µm. Cells were pre-treated with pertussis toxin (PTX; 200 ng/ml, over night) or YM-254890 (1 µM, for 15 min prior to GPCR stimulation or 5 h when stimulated with PMT). Stimulation of the cells with the toxin was performed for 5 h at a concentration of 1 nM PMT. In order to stimulate the GPCRs, the cells were treated with 1 µM fMLP (Merck) or 100 µM carbachol (Sigma) for 2–5 min.

2.5. Semi-quantitative analysis of GFP-Grp1PH translocation

The GFP-labeled PH domain of the general receptor for phosphoinositides-1 (GFP-Grp1_{PH}) binds specifically to PIP₃ [23]. Therefore the subcellular distribution of GFP-Grp1_{PH} reflects the activity of PI3Ks, i.e. enhancement of membrane-associated fluorescence was taken as an indicator of PI3K activation.

For semi-quantitative analysis of PI3K activation in PMT pre-treated cells the ratio of the fluorescence intensities of GFP-Grp1_{PH} at the cell surface and the cell interior of the confocal plane were calculated ($F_{\text{mbre}}/F_{\text{cyto}}$) and compared to control cells. F_{mbre} represents the mean intensity of fluorescence per µm² associated with the plasma membrane compartment whereas F_{cyto} represents the mean intensity of the intracellular fluorescence per µm². For statistical analysis of PI3K activity means and standard deviations were calculated from three independent experiments based on different transfections analyzing six cells each.

The semi-quantitative evaluation of the kinetics of receptor-induced PI3K activation was not based on the increasing fluorescence intensity at the membrane since values quickly reached saturation. Instead, we measured the simultaneous decrease of the cytosolic fluorescence intensity. This approach is based on the assumption that the disappearance of GFP-Grp1_{PH}-dependent fluorescence from the cytosol is almost completely due to its translocation to the plasma membrane except for the bleaching effect which is covered by control experiments. Accordingly, shortly before and after application of the stimulus successive pictures were taken (every 10 s for 3–4 min).

The relative amount of GFP-Grp1_{PH} domain translocated at the time (t) is given by this equation: relative PI3K activity = $[(F_{\text{cyto}}(0) - F_{\text{cyto}}(t))/F_{\text{cyto}}(0)] \times 100$.

$F_{\text{cyto}}(0)$ represents the cytosolic fluorescence immediately before stimulation. $F_{\text{cyto}}(t)$ represents the cytosolic fluorescence at time (t) after stimulation. For statistical analysis of PI3K activity means and standard deviations were calculated for six cells from independent transfections.

Statistical significance was assessed using a paired Student's t -test, with * $p < 0.05$, ** $p < 0.01$ and *** $p < 0.005$.

2.6. Site-directed mutagenesis

Mutations were introduced by site-directed mutagenesis, using G α_q cloned into pLNXC2 as template [8] and the respective oligonucleotides, using the Quick-Change kit, according to the manufacturer's instructions. From the two complementary primers used for each mutation, only one is listed: G α_q ^{G208A}, 5'-GTC GAT GTA GGG GCC CAA AGG TCA GAG A-3'; G α_q ^{I25A/E26A}, 5'-ATC AAC GAC GAG GCC GCG CGG CAC GTG CGC-3'; GRK2-CT^{R587Q}, 5'-CCT GTT CCC TAA CCA GCT CGA GTG GCG GGG C-3'. All mutations were confirmed by DNA sequencing with the ABI PRISM™ Dye Terminator Cycle Sequencing Ready Reaction kit (Perkin Elmer).

2.7. Assay of SRF activation

HEK293-M₃ cells were transfected with the pSRE.L-luciferase reporter plasmid and the pRL.TK control reporter vector. pSRE.L encodes for firefly (*Photinus pyralis*) luciferase; the expression is induced by activation of SRF. pRL.TK encodes for *Renilla* (*Renilla reniformis*) luciferase, which is expressed constitutively. The plasmids pSRE.L and pRL.TK were kind gifts of Dr. R. Treisman (Transcription Laboratory, Imperial Cancer Research Fund Laboratories, London, England). Cells were transfected using the jetPEI-transfection Kit from Biomol. Cultures were serum-starved for 24 h before stimulation with PMT for additional 20 h and lysed with passive lysis buffer (Promega). Luciferase activities were determined with the Dual-Luciferase reporter assay system (Promega) in accordance to the manufacturer's instructions. The activity of the experimental reporter was normalized against the activity of the control vector.

2.8. Analysis of total inositol phosphates

G $\alpha_{q/11}$ -deficient MEF transduced with retroviral constructs were grown in 24-well plates for 2 to 3 days. Then, cultures were labeled

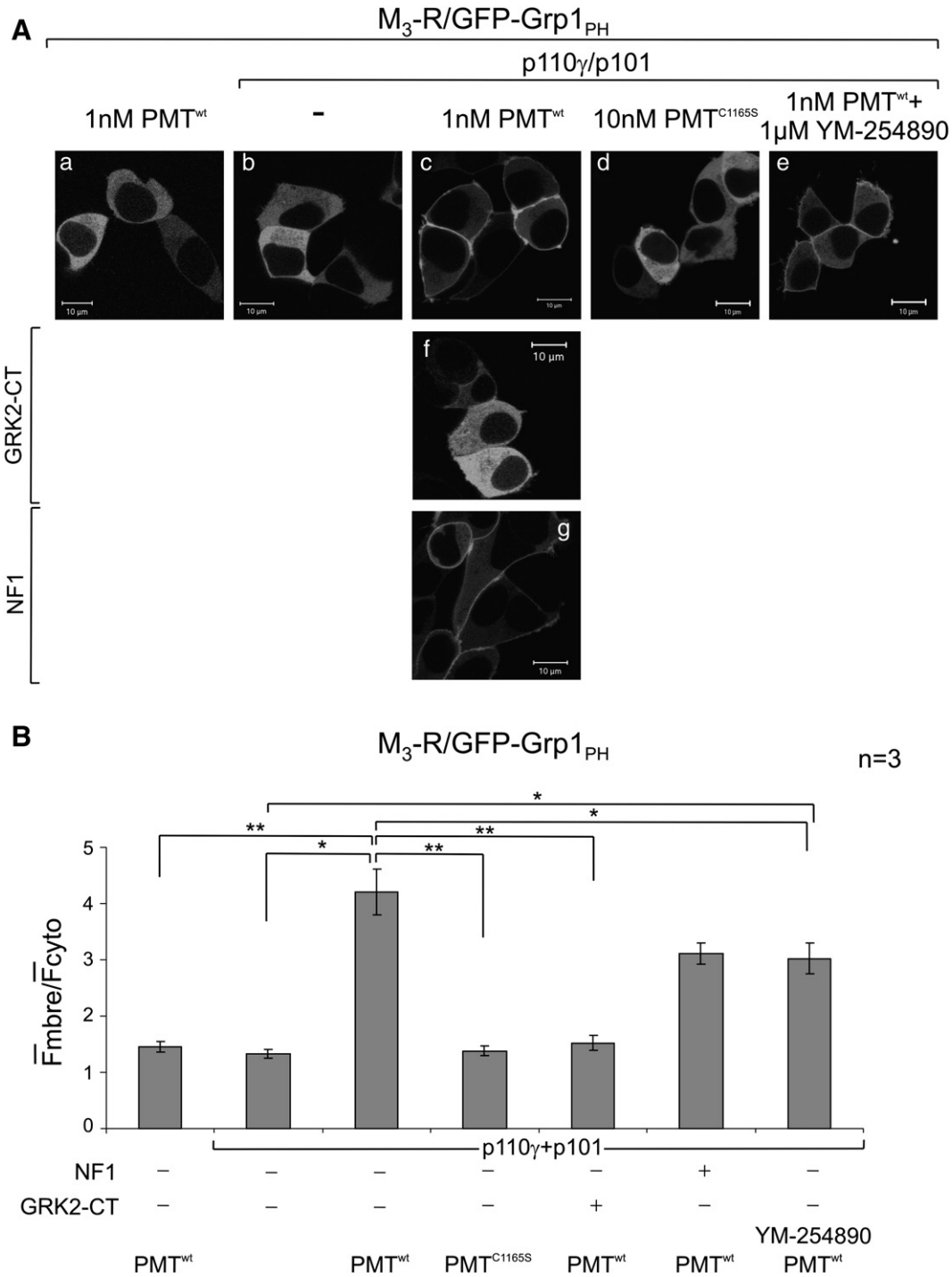


Fig. 1. PMT leads to G $\beta\gamma$ -dependent activation of the PI3K γ in HEK293-M₃ cells. A. In each set of parallel experiments HEK293-M₃ cells were transfected with the identical mixture of plasmids as indicated in the figure. Treatment of cells was without (b) and with wild-type PMT (a, c, f and g, 1 nM PMT^{wt}), inactive PMT mutant (d, 10 nM PMT^{C1165S}) and wild-type PMT plus compound YM-254890 (e, 1 nM, PMT^{wt} + 1 μ M YM-254890) for 5 h. In f, the effect of the G $\beta\gamma$ -scavenger GRK2-CT is shown; g shows the effect of the Ras-GAP NF1. B. Histogram showing the quantification of the membrane translocation of GFP-Grp1_{PH} from (A). The membrane translocation of GFP-Grp1_{PH} is evaluated as the ratio: F_{mbre}/F_{cyto} (mean intensity of fluorescence per μm^2 associated with the membrane/mean intensity of intracellular fluorescence per μm^2 ; for details see “Experimental Procedures” section). Data depicted represent the mean \pm SD of 3 independent sets of experiments analyzing 18 cells. Statistical significance was assessed using a paired Student’s *t*-test, with **p* < 0.05 and ***p* < 0.01.

with 2 $\mu\text{Ci}/\text{ml}$ of [2-³H]inositol in inositol- and serum-free medium over night. PMT was added at the indicated concentration and incubated for the indicated time. LiCl (20 mM) was added 60 min before assay was stopped to allow accumulation of inositol phosphates. Thereafter, the medium was replaced by 750 μl of ice-cold formic acid (10 mM, pH 3). After 30 min, the extract was neutralized with 3 ml of NH₃ (5 mM, pH 8–9). Analysis of total inositol phosphates

was done by anion exchange chromatography as described before [24].

2.9. Expression of recombinant proteins

Recombinant PMT^{wt} and the inactive mutant PMT^{C1165S} were expressed and purified as described before [24].

2.10. Immunoblot analysis

Cells were extracted at 4 °C with RIPA buffer (50 mM Hepes, pH 7.4, 150 mM NaCl, 5 mM MgCl₂, 1 mM EDTA, 1% Nonidet P-40, 0.5% (w/v) deoxycholate, 0.1% (w/v) SDS, and complete protease inhibitors, Roche Applied Science) and analyzed by Western-blotting after SDS-polyacrylamide gel electrophoresis. Anti Gα_{q/11}-, anti flag-M2 and anti GRK2-CT antibodies were purchased from Santa Cruz Biotechnology, Sigma and Epitomics, respectively. Binding of the second horseradish peroxidase-coupled antibody was detected with enhanced chemiluminescent detection reagent (100 mM Tris-HCl, pH 8.0, 1 mM luminol (Fluka), 0.2 mM p-coumaric acid, and 3 mM H₂O₂), and the imaging system LAS-3000 (Fujifilm).

3. Results

3.1. Activation of PI3Kγ by PMT

It has been shown that PMT activates G_q in a receptor-independent manner [11]. This results in activation of PLC-β by Gα_q [9,11]. To study whether PMT induces not only activation of Gα- but also of Gβγ-dependent pathways, we transfected HEK293 cells stably expressing the G_q-coupled M₃ receptor (Fig. S2B) with plasmids encoding a heterodimeric PI3Kγ, a prototypical Gβγ effector, which is not endogenously expressed in HEK cells [14,25,26]. Activation of PI3Kγ was assessed by translocation of the PIP₃-sensor GFP-Grp1_{PH} from the cytosol to the membrane (Fig. 1). In the absence of PI3Kγ PMT (1 nM) had no effect on redistribution of GFP-Grp1_{PH} indicating that the

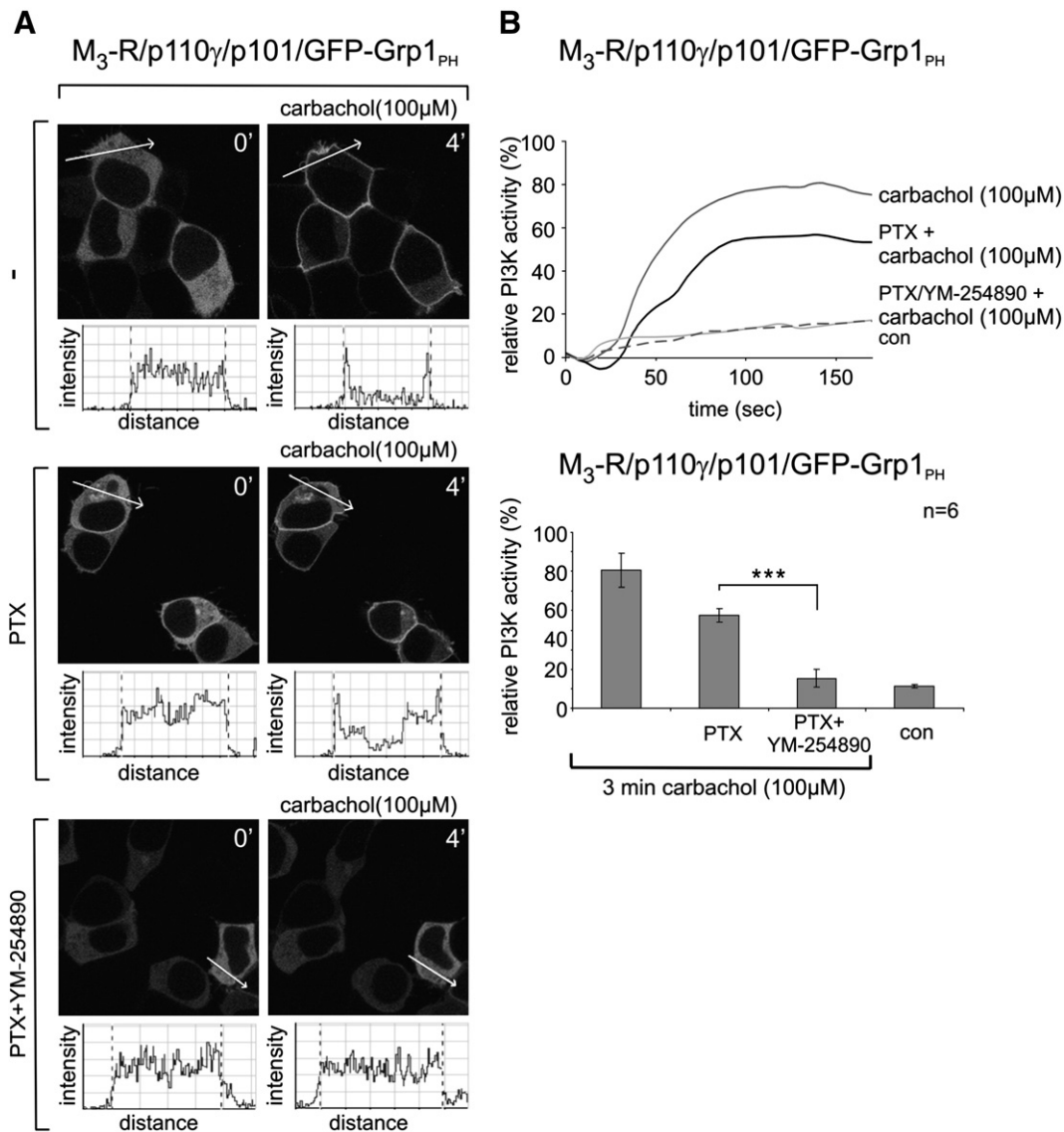


Fig. 2. Ability of PTX and compound YM-254890 to inhibit the M₃ receptor-mediated activation of PI3Kγ. **A.** In each set of parallel experiments HEK293-M₃ cells were co-transfected with the identical mixture of plasmids, encoding for p110γ, p101 and GFP-Grp1_{PH}, starved for 24 h and stimulated with carbachol (100 μM). Shown are confocal images of representative cells before and after 4 min of stimulation with carbachol. In the large upper panel, the activity of the PI3Kγ upon muscarinic acetylcholine receptor M₃ stimulation is shown. The large middle panel shows GFP-Grp1_{PH} redistribution before and after carbachol stimulation (100 μM, 4 min) in cells pretreated with pertussis toxin (PTX, 200 ng/ml, overnight). Large lower panel shows GFP-Grp1_{PH} redistribution before and after carbachol (100 μM, 4 min) in cells treated with both, pertussis toxin (PTX, 200 ng/ml, over night) and the G_q-protein inhibitor YM-254890 (1 μM, added 15 min before carbachol). The small panels show the intensity of fluorescence measured along the arrows indicated in the large panels. **B.** Kinetics and histogram of GFP-Grp1_{PH} membrane translocation from the experiments shown in (A). The kinetic representation of the activation process in the cells depicted in (A) shows the time dependency of the PH domain redistribution over 3 min (note: endpoint in A was after 4 min). The histogram shows means ± SD of the fluorescence at the membrane for six cells after 3 min of activation by carbachol (100 μM). Statistical significance was assessed using a paired Student's *t*-test, with ****p* < 0.005.

and a Ras activity assay (Fig. S2A). These findings indicate that PMT signals not only via $G\alpha_q$ but also via $G\beta\gamma$.

3.2. Involvement of different G proteins in PI3K activation by PMT

Recently, we reported that also G_i is potently activated by PMT [12]. To test whether G_q is the only source of PMT-released $G\beta\gamma$ dimers, we used the $G\alpha_q$ -inhibitor YM-254890, which prevents activation of G_q not only by receptors but also by PMT [30,31]. For control, it was initially confirmed that YM-254890 inhibited $G\beta\gamma$ signaling from GPCR-activated $G\alpha_q\beta\gamma$ complex (Fig. 2). To this end, the effects of the muscarinic agonist carbachol were studied on GFP-Grp1_{PH} translocation. As shown in Fig. 2, carbachol-activated M_3 receptor caused a rapid translocation of GFP-Grp1_{PH}. This effect was partially blocked by pretreatment with pertussis toxin (PTX), which completely inhibited G_i activation as confirmed in parallel experiments (see also supplementary information indicating that PTX treatment completely blocked G_i signaling via fMLP receptors; Fig. S1). Addition of YM-254890 to PTX-pretreated cells completely blocked translocation, indicating the involvement of G_i and G_q in the effect by carbachol. Interestingly, PMT-induced stimulation of PI3K γ was only partially affected by the G_q inhibitor YM-254890 (Fig. 1), suggesting the involvement of additional G protein isoforms beside G_q such as G_i . In the case of PMT we could not use PTX to identify G_i as an additional source for $G\beta\gamma$, because it is known that PMT activates G_i even after ADP-ribosylation by PTX [12].

Similar results were obtained in HEK293 cells without stable expression of the M_3 receptor (Fig. 3). For semi-quantitative comparison of PMT-induced PI3K γ activity $G\beta\gamma$ was transfected in HEK cells which elicits maximal stimulation of the enzyme. Only a slightly higher activity of PI3K γ was observed in cells over-expressing $G\beta\gamma$ compared to PMT-treated cells (Fig. 3B).

3.3. $G\beta\gamma$ is essential for activation of G proteins by PMT

As our studies suggested that $G\beta\gamma$ subunits play a crucial role in PI3K activation by PMT, we investigated the effects of the toxin on $G\beta\gamma$ release (activation) in more detail. For this purpose we employed mutant $G\alpha_q$ proteins, which are known to be defective in $G\beta\gamma$ cycling. The $G\alpha_q$ double mutant I25A/E26A has lost its ability to bind the $G\beta\gamma$ -dimers [32,33]. In contrast, the G208A mutant of $G\alpha_q$ is known to permanently bind $G\beta\gamma$ and is not able to release $G\beta\gamma$ upon G_q interaction with agonist-bound receptors [34–36]. The mutant proteins were expressed in MEF cells, which were defective of $G\alpha_{q/11}$. The amount of protein expressed was verified by Western-blotting (Fig. 4C). As a control, we studied the effects of phenylephrine, which is an agonist at α_1 -adrenoceptors. As expected, phenylephrine did not increase inositol phosphate accumulation in $G\alpha_{q/11}$ -deficient MEF. In contrast, after transfection of $G\alpha_q$, phenylephrine stimulated inositol phosphate accumulation in cells expressing wild-type $G\alpha_q$ about 3-fold. Stimulation of inositol phosphate accumulation was lost when the $G\alpha_q$ mutants G208A or I25A/E26A were transfected. Similarly, PMT potently stimulated inositol phosphate accumulation following expression of wild-type $G\alpha_q$ in $G\alpha_{q/11}$ -deficient MEFs. As observed for GPCR-mediated effects of phenylephrine, the $G\alpha_q$ mutants G208A or I25A/E26A did not allow stimulation of inositol phosphate accumulation by PMT-treatment, indicating the essential role of $G\beta\gamma$ (Fig. 4B). These findings suggest that cycling of $G\beta\gamma$ dimers is essential for the action of PMT, because both mutants of $G\alpha_q$ that one, which permanently binds $G\beta\gamma$ subunits (G208A), and that one, which is not able to bind $G\beta\gamma$ (I25A/E26A), were not activated by PMT.

Next, we studied the role of $G\beta\gamma$ on PMT-induced, Rho-dependent activation of serum responsive factor, which was shown to be mediated by G_q and/or $G_{12/13}$ [31]. For this purpose Rho- and SRF-dependent luciferase activation was measured in the presence and absence of GRK2-CT. As a control, effects of the muscarinic (M_3)

receptor agonist carbachol were compared with PMT. As shown in Fig. 5A, carbachol- and PMT-induced activation of luciferase activity was strongly reduced by co-expression of GRK2-CT. The GRK-2 mutant (R587Q) of the C-terminal fragment (Fig. S2C), which does not sequester $\beta\gamma$ subunits [37], did not inhibit PMT-induced luciferase activation. Fig. 5B shows the concentration dependency of the inhibiting effect of the C-terminus of GRK2. Increasing expression of GRK2-CT inhibited Rho-dependent luciferase activity stimulated by PMT. In addition, we examined the effect of phosducin, which is another scavenger of $G\beta\gamma$ proteins [38–40]. Over-expression of phosducin inhibited muscarinic receptor-mediated SRF-dependent luciferase activity (Fig. 5C and D) and, similarly, increase in luciferase activity caused by PMT treatment of cells was inhibited by phosducin.

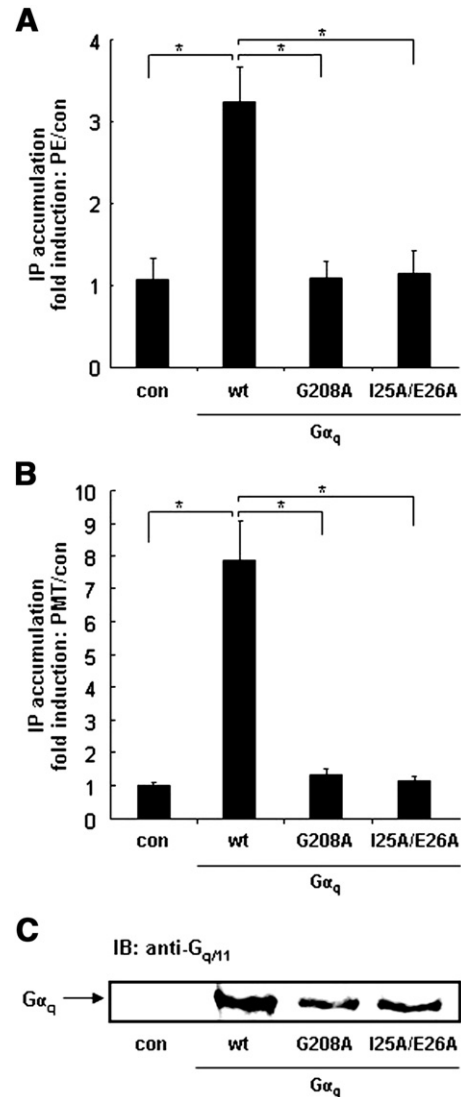


Fig. 4. Mutants of $G\alpha_q$, affecting $G\beta\gamma$ binding, block PMT-induced activation of $G\alpha_q$ -PLC β pathway. $G\alpha_q^{wt}$, $G\alpha_q^{G208A}$ or $G\alpha_q^{I25A/E26A}$ encoding retrovirus was produced and $G\alpha_q/G\alpha_{11}$ -deficient MEF were transfected with resulting retrovirus as described under "Experimental Procedures". Additional transfection of α_1 -adrenoceptor expression plasmid was done with the Nucleofection system (Amaxa Biosystems). Transfected MEF were stimulated with 10 μ M phenylephrine (PE) for 30 min (panel A) or with 10 nM PMT for 6 h (panel B). The total amount of inositol phosphates was measured as described under "Experimental Procedures". *, indicates significant difference ($p < 0.005$) calculated with ANOVA. Data are given as fold induction over buffer control (mean \pm SEM; $n = 3$). C. Expression of $G\alpha_q^{wt}$, $G\alpha_q^{G208A}$ or $G\alpha_q^{I25A/E26A}$ in retroviral transfected $G\alpha_q/G\alpha_{11}$ -deficient MEF was examined by Western-blotting. Shown is an immunoblot of RIPA-extracts of $G\alpha_q/G\alpha_{11}$ -deficient cells. The immunoblot was performed as described under "Experimental Procedures".

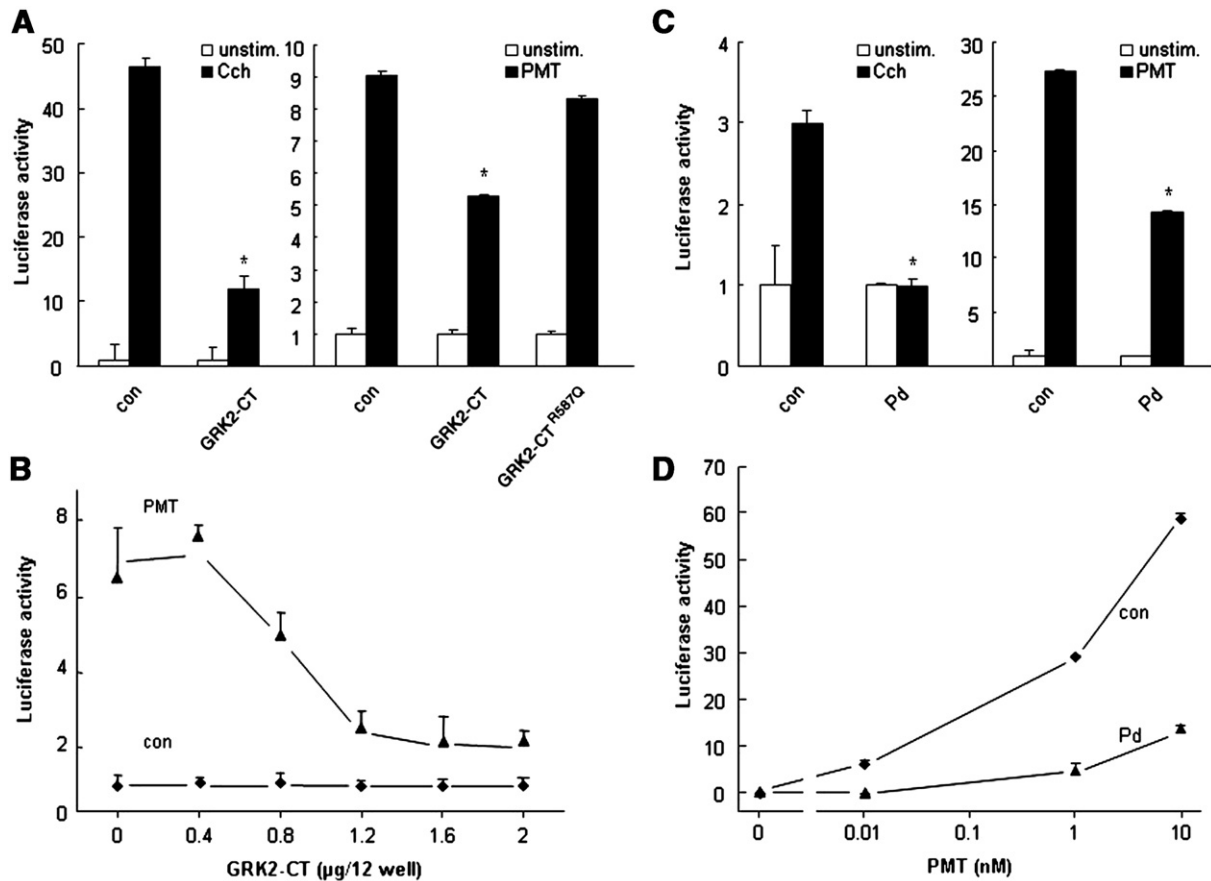


Fig. 5. Sequestration of G $\beta\gamma$ subunits inhibits PMT-induced activation of SRE-dependent luciferase expression. **A.** Luciferase production was measured in HEK293-M $_3$ cells transfected with pSRE.L, pRL.TK and control vectors alone (*con*), GRK2-CT or GRK2-CT^{R587Q} (each 50 ng of DNA per well). Cells were stimulated for 24 h with 1 mM carbachol (Cch, black bars, left part), 1 nM PMT (black bars, right part) or left unstimulated (white bars). Given is the fold stimulation of luciferase as compared to controls. *, indicates significant difference between stimulated values ($p < 0.005$) calculated with ANOVA. **B.** Luciferase production was measured in HEK293-M $_3$ cells transfected with pSRE.L, pRL.TK and increasing amounts of GRK2-CT. The total amount of transfected cDNA was always kept constant by the addition of empty expression vector. Cells were stimulated for 24 h with 1 nM PMT (triangle) or left unstimulated (rhombus). **C.** Luciferase production was measured in HEK293-M $_3$ cells transfected with pSRE.L, pRL.TK and control vectors alone (*con*) or phosducin (Pd, each 50 ng of DNA per well). Cells were stimulated for 24 h with 1 mM carbachol (Cch, black bars, left part), 1 nM PMT (black bars, right part) or left unstimulated (white bars). *, indicates significant difference between stimulated values ($p < 0.005$) calculated with ANOVA. **D.** Luciferase production was measured in HEK293-M $_3$ cells transfected with pSRE.L, pRL.TK and control vectors alone (*con*, rhombus) or phosducin (PD, triangle) (each 50 ng of DNA per well). Cells were stimulated for 24 h with increasing concentration of PMT as indicated. Given is the fold stimulation of luciferase as compared to controls. Data are given as mean \pm SEM ($n = 4$).

This inhibiting effect was observed over a wide concentration range of PMT (Fig. 5D).

4. Discussion

PMT is a potent GPCR-independent activator of G α_q and G α_i proteins [11]. Here we addressed the question, whether toxin-induced activation of G proteins also results in activation of G $\beta\gamma$. To this end, the activation of PI3K γ , which is an established effector of G $\beta\gamma$ [14,25,26], was analyzed after treatment of cells with PMT. As a read out for activation of PI3K, we investigated the translocation of GFP-Grp1_{PH} from the cytosol to membranes. Due to its PH domain, the GFP-Grp1_{PH} protein binds to PIP $_3$, which is a product of PI3K and is located in the membrane. We show that after over-expression of p110 γ /p101 (PI3K γ), PMT caused a strong and specific translocation of GFP-Grp1_{PH} from the cytosol to membranes, indicating the activation of PI3K γ . These findings were corroborated by sequestration experiments with GRK2-CT. The C-terminal part of GRK-2 is known to bind G $\beta\gamma$ thereby preventing signaling via G $\beta\gamma$ [28,29]. GRK2-CT effectively blocked PMT-induced translocation of GFP-Grp1_{PH}, supporting the notion that G $\beta\gamma$ subunits are responsible for PMT-induced activation of PI3K γ . Because PI3K γ is also activated via Ras [27], we excluded a significant involvement of Ras in PMT-induced activation of PI3K γ by over-

expression of NF1, which inactivates Ras proteins by its GAP (GTPase-activating) function.

One major target of PMT is G $_q$. However, the G $_q$ inhibitor YM-254890 only partially blocked PMT-induced translocation of GFP-Grp1_{PH}, suggesting that also other G protein isoforms are involved. Release of G $\beta\gamma$ from G $_i$ has been shown to cause PI3K activation [14]. We reported recently that not only G $_q$ and G $_{12/13}$ but also G $_i$ is activated by PMT [12]. Therefore, G $_i$ is most likely another source of PMT-induced G $\beta\gamma$ release. Notably, PMT-induced activation of G α_i is not inhibited by PTX [12].

As our translocation studies suggested that PMT causes release of G $\beta\gamma$, we were prompted to analyze the general role of G $\beta\gamma$ in activation of G proteins by PMT. Therefore, PMT-induced inositol phosphate accumulation and Rho-dependent SRF-activation were studied in the presence of the G $\beta\gamma$ scavengers GRK2-CT, which resulted in inhibition of PMT-induced activation of G protein effects. Inhibition of PMT-induced effects on G proteins by sequestration of G $\beta\gamma$ was confirmed by using phosducin, which is another protein that sequesters G $\beta\gamma$ [38–40].

Two well characterized mutants of G α_q (I25A/E26A and G208A) were employed to study the role of G $\beta\gamma$ in more detail. The double mutant G $\alpha_q^{I25A/E26A}$ is not able to bind G $\beta\gamma$ [33,41], whereas G α_q^{G208A} interacts with high affinity with G $\beta\gamma$ subunits [34–36]. With both

mutants, the PMT-induced activation of G_q was blocked. These findings suggest that the cycling of $G\beta\gamma$, e.g. the association with and/or dissociation from $G\alpha_q$, is essential for the action of the toxin on G proteins. This is surprising, because it has been shown that at least the C-terminus of $G\alpha$, which is essential for interaction with GPCRs, is not needed for PMT-induced activation of G proteins [11]. Recently we showed that PMT causes inhibition of the GTPase activity and uncouples G_i from activating receptors [12]. Because $G\beta\gamma$ subunits are not directly involved in the GTPase activity of G proteins, we speculate that it is necessary for loading of the G protein with GTP. However, our findings cannot exclude that the mutations (e.g., I25A/E26A and G208A) of G_q affect the interaction of PMT or the interaction of a cellular regulator (e.g. RGS) with the G protein.

5. Conclusion

Taken together, here we show that PMT-induced activation of heterotrimeric G proteins leads not only to signaling of the α subunit but also to release of $G\beta\gamma$. By a pharmacological approach we could show that G_q is not the only source of $G\beta\gamma$. Also PMT-activated G_i contributes to $G\beta\gamma$ release. Additionally, we show that $G\beta\gamma$ plays an important role in PMT-induced activation and signaling of the G proteins.

Acknowledgements

This study was financially supported by the DFG (SFB 746 to K.A., and NU53/6-1 and TP2, FOR 729 to B.N.). We thank Dr. M.R. Ahmadian, Düsseldorf, for kindly providing the flag-NF1-333 plasmid and GST-RBD lysates, Dr. S. Offermanns for the kind gift of $G\alpha_q/G\alpha_{11}$ -deficient MEF; Dr. Masatoshi Taniguchi for the inhibitor YM-254890 and Silke Fieber and Petra Bartholomè for excellent technical assistance.

Appendix A. Supplementary data

Supplementary data associated with this article can be found, in the online version, at doi:10.1016/j.cellsig.2008.12.007.

References

- [1] B.A. Wilson, M. Ho, *Pasteurella multocida* toxin, in: J.E. Alouf, M.R. Popoff (Eds.), *The Comprehensive Sourcebook of Bacterial Protein Toxins*, Elsevier, Amsterdam, 2006, p. 430.
- [2] M.A. Dominick, R.B. Rimler, *Am. J. Vet. Res.* 47 (1986) 1532.
- [3] M. Harper, J.D. Boyce, B. Adler, *FEMS Microbiol. Lett.* 265 (2006) 1.
- [4] E. Rozengurt, T. Higgins, N. Chanter, A.J. Lax, J.M. Staddon, *Proc. Natl. Acad. Sci. U. S. A.* 87 (1990) 123.
- [5] L.I. Dudet, P. Chailier, D. Dubreuil, B. Martineau-Doize, *J. Cell. Physiol.* 168 (1996) 173.
- [6] B. Seo, E.W. Choy, W.E. Maudsley, W.E. Miller, B.A. Wilson, L.M. Luttrell, *J. Biol. Chem.* 275 (2000) 2239.
- [7] J.H. Orth, K. Aktories, K.F. Kubatzky, *J. Biol. Chem.* 282 (2007) 3050.
- [8] J.H. Orth, S. Lang, K. Aktories, *J. Biol. Chem.* 279 (2004) 34150.
- [9] B.A. Wilson, X. Zhu, M. Ho, L. Lu, *J. Biol. Chem.* 272 (1997) 1268.
- [10] A. Zywiets, A. Gohla, M. Schmelz, G. Schultz, S. Offermanns, *J. Biol. Chem.* 276 (2001) 3840.
- [11] J.H. Orth, S. Lang, I. Preuss, G. Milligan, K. Aktories, *Cell. Signal.* 19 (2007) 2174.
- [12] J.H. Orth, I. Fester, I. Preuss, L. Agnoletto, B.A. Wilson, K. Aktories, *J. Biol. Chem.* 283 (2008) 23288.
- [13] K. Kitadokoro, S. Kamitani, M. Miyazawa, M. Hanajima-Ozawa, A. Fukui, M. Miyake, Y. Horiguchi, *Proc. Natl. Acad. Sci. U. S. A.* 104 (2007) 5139.
- [14] C. Brock, M. Schaefer, H.P. Reusch, C. Czupalla, M. Michalke, K. Spicher, G. Schultz, B. Nürnberg, *J. Cell Biol.* 160 (2003) 89.
- [15] M.R. Ahmadian, U. Hoffmann, R.S. Goody, A. Wittinghofer, *Biochemistry* 36 (1997) 4535.
- [16] P. Voigt, M.B. Dorner, M. Schaefer, *J. Biol. Chem.* 281 (2006) 9977.
- [17] C. Klenk, J. Humrich, U. Quitterer, M.J. Lohse, *J. Biol. Chem.* 281 (2006) 8357.
- [18] J.M. Lopez De, M.B. Stope, P.A. Oude Weernink, Y. Mahlke, C. Borgermann, V.N. Ananaba, C. Rimmbach, D. Roskopf, M.C. Michel, K.H. Jakobs, M. Schmidt, *J. Biol. Chem.* 281 (2006) 21837.
- [19] S. Vogt, R. Grosse, G. Schultz, S. Offermanns, *J. Biol. Chem.* 278 (2003) 28743.
- [20] C. Nickel, T. Benzing, L. Sellin, P. Gerke, A. Karihaloo, Z.-X. Liu, L.G. Cantley, G. Walz, *J. Clin. Invest.* 109 (2002) 481.
- [21] P. Voigt, C. Brock, B. Nürnberg, M. Schaefer, *J. Biol. Chem.* 280 (2005) 5121.
- [22] L. Schneider, F. Essmann, A. Kletke, P. Rio, H. Hanenberg, W. Wetzel, K. Schulze-Osthoff, B. Nürnberg, R.P. Piekorz, *J. Biol. Chem.* 282 (2007) 29273.
- [23] C.P. Downes, A. Gray, J.M. Lucocq, *Trends Cell Biol.* 15 (2005) 259.
- [24] C. Busch, J. Orth, N. Djouder, K. Aktories, *Infect. Immun.* 69 (2001) 3628.
- [25] U. Maier, A. Babich, B. Nürnberg, *J. Biol. Chem.* 274 (1999) 29311.
- [26] L.R. Stephens, A. Eguinoa, H. Erdjument-Bromage, M. Lui, F. Cooke, J. Coadwell, A.S. Smrcka, M. Thelen, K. Cadwallader, P. Tempst, P.T. Hawkins, *Cell* 89 (1997) 105.
- [27] S. Suires, P. Hawkins, L. Stephens, *Curr. Biol.* 12 (2002) 1068.
- [28] W.J. Koch, B.E. Hawes, J. Inglese, L.M. Luttrell, R.J. Lefkowitz, *J. Biol. Chem.* 269 (1994) 6193.
- [29] M. Sallese, S. Mariggio, E. D'Urbano, L. Iacovelli, B.A. De, *Mol. Pharmacol.* 57 (2000) 826.
- [30] J. Takasaki, T. Saito, M. Taniguchi, T. Kawasaki, Y. Moritani, K. Hayashi, M. Kobori, *J. Biol. Chem.* 279 (2004) 47438.
- [31] J.H. Orth, S. Lang, M. Taniguchi, K. Aktories, *J. Biol. Chem.* 280 (2005) 36701.
- [32] D.S. Evanko, M.M. Thiyagarajan, P.B. Wedegaertner, *J. Biol. Chem.* 275 (2000) 1327.
- [33] D.S. Evanko, M.M. Thiyagarajan, S. Takida, P.B. Wedegaertner, *Cell. Signal.* 17 (2005) 1218.
- [34] E. Lee, R. Taussig, A.G. Gilman, *J. Biol. Chem.* 267 (1992) 1212.
- [35] J.J. Carrillo, J. Padiani, G. Milligan, *J. Biol. Chem.* 278 (2003) 42578.
- [36] B. Barren, N.O. Artemyev, *J. Neurosci. Res.* 85 (2007) 3505.
- [37] C.V. Carman, L.S. Barak, C. Chen, L.Y. Liu-Chen, J.J. Onorato, S.P. Kennedy, M.G. Caron, J.L. Benovic, *J. Biol. Chem.* 275 (2000) 10443.
- [38] P.H. Bauer, S. Müller, M. Puzicha, S. Pippig, B. Obermaier, E.J.M. Helmreich, M.J. Lohse, *Nature* 358 (1992) 73.
- [39] S. Schroder, M.J. Lohse, *Proc. Natl. Acad. Sci. U. S. A.* 93 (1996) 2100.
- [40] K. Bluml, W. Schnepf, S. Schroder, M. Beyermann, M. Macias, H. Oshkinat, M.J. Lohse, *EMBO J.* 16 (1997) 4908.
- [41] A. Jetzt, J.A. Howe, M.T. Horn, E. Maxwell, Z. Yin, D. Johnson, C.C. Kumar, *Cancer Res.* 63 (2003) 6697.